IIETA International Information and Engineering Technology Association
Advancing the World of Information and Engineering

Journal Européen des Systèmes Automatisés
Vol. 53, No. 6, December, 2020, pp. 825-834
Journal homepage: http://iieta.org/journals/jesa

Proxy-Based Sliding Mode Vibration Control with an Adaptive Approximation Compensator for Euler-Bernoulli Smart Beams

Hayder F.N. Al-Shuka

Department of Aeronautical Engineering, University of Baghdad, Baghdad 10001, Iraq

Corresponding Author Email: hayder.al-shuka@rwth-aachen.de

https://doi.org/10.18280/jesa.530608

Received: 29 June 2020
Accepted: 24 November 2020

Keywords:
proxy-based sliding mode control, piezo-patches, Euler-Bernoulli beam, adaptive approximation technique

ABSTRACT

Proxy-based sliding mode control PSMC is an improved version of PID control that combines the features of PID and sliding mode control SMC with continuously dynamic behaviour. However, the stability of the control architecture maybe not well addressed. Consequently, this work is focused on modification of the original version of the proxy-based sliding mode control PSMC by adding an adaptive approximation compensator AAC term for vibration control of an Euler-Bernoulli beam. The role of the AAC term is to compensate for unmodelled dynamics and make the stability proof more easily. The stability of the proposed control algorithm is systematically proved using Lyapunov theory. Multi-modal equation of motion is derived using the Galerkin method. The state variables of the multi-modal equation are expressed in terms of modal amplitudes that should be regulated via the proposed control system. The proposed control structure is implemented on a simply supported beam with two piezo-patches. The simulation experiments are performed using MATLAB/SIMULINK package. The locations of piezo-transducers are optimally placed on the beam. A detailed comparison study is implemented including three scenarios. Scenario 1 includes disturbing the smart beam while no feedback loop is established (open-loop system). In scenario 2, a PD controller is applied on the vibrating beam. Whereas, scenario 3 includes implementation of the PSMC+AAC. For all previously mentioned scenarios, two types of disturbances are applied separately: 1) an impulse force of 1 N peak and 1 s pulse width, and 2) a sinusoidal disturbance with 0.5 N amplitude and 20 Hz frequency. For impulse disturbance signals, the results show the superiority of the PSMC+AAC in comparison with the conventional PD control. Whereas, both the PSMC+ACC and the PD control work well in the case of a sinusoidal disturbance signal and the superiority of the PSMC is not clear.

1. INTRODUCTION

Much attention has been paid to active vibration control of flexible structures. These structures have been widely used in miscellaneous applications such as space robotics, aircraft structures, gas turbine rotors, skyscrapers, and bridges [1-4]. They may damage if they undergo unwanted vibrational loads because of possible fatigue and instability. Therefore, they need a suitable control system to suppress the vibrational motion and maintain structural stability. The use of smart materials as actuators and/or sensors witnesses progress in practice and research fields proving a potential solution to reduce the failure of the structures. A smart beam-like structure consists of a regular beam with attached distributed smart materials behaving as actuators and/or sensors. They can actively suppress produced oscillations instead of using passive damping parts [5]. As a result, this work is concerned with modelling and control of slender beams with surface bonded piezo-patches (actuators/sensors). Design of a suitable control architecture requires good mathematical modelling for the target dynamic system. In general, three beam theories have been reported in the literature: Euler-Bernoulli theory that neglects the rotational inertia and shear deformation, Rayleigh theory that considers the shear deformation only while Timoshenko beam theory considers both the rotational inertia and shear deformation [6-8]. The current work is focused on an Euler-Bernoulli beam model with attached piezo-materials. The vibrating beam has infinite degrees-of-freedom with a large number of vibrational modes. However, the objective of the designed controller is to stabilize the vibration of the first mode shapes since they are dominant in the low-frequency region of the dynamic response. Therefore, the partial differential equation PDF is transformed into discrete ordinary differential equations ODEs with a definite number of mode shapes.

Miscellaneous control approaches have been used for vibration control of smart flexible beams such as strain rate feedback [9], positive position feedback [10], pulse frequency modulator [11], PID controller [12], Linear quadratic regulator (LQR), state feedback [13], model predictive control [14], and more recent works [15-20]. However, the performance and stability of the above-mentioned control schemes could be corrupted if undesired external disturbances are applied or unmodeled dynamics are neglected. Above all, the PID family controller has a simple structure but it can work well at the low-frequency region; the control system performance could be destabilized beyond the cut-off frequency [21]. To overcome PID limitations, a feedforward term is added to the PID term to obtain high bandwidth control. However, if the dynamic modelling includes uncertainties, the adaptive

control is integrated such that the parameters associated with the feedforward term are updated based on Lyapunov theory [22-33]. In effect, there are two basic strategies for adaptive control: regressor-based control and approximation-based control. In contrast to the regressor approach, the adaptive approximation technique is a model-free control includes representation of the uncertainties in terms of weighting and basis function vectors/matrices. The weighting coefficients are updates based on Lyapunov theory, see the papers [22-33] for more details. However, modelling error should be compensated by using a robust sliding term. The sliding mode control is a powerful robust control strategy for stabilization of motion of dynamic systems with uncertain modelling. It includes a nonlinear discontinuous function, e.g. signum-type function, to enforce the state variables approaching to the sliding surface (modelling and position errors are convergent to zero). However, due to the presence of a discontinuous signum function in the closed-loop dynamics, this could lead to chattering problem and hence stability and performance of the sliding mode control can be degraded. Chattering problem can cause high-frequency dynamics with large position error [34]. In general, there are three approaches for attenuation of chattering problem: 1) boundary layer method [35], 2) high order sliding control [36], and 3) proxy-based sliding control [37]. Boundary layer method replaces the discontinuous signum function by a continuous function, e.g. a saturated function or a hyperbolic tangent function, etc. However, due to the presence of approximation error, the stability of the control system can be degraded. On the other hand, high order sliding mode control requires a state observer to estimate derivatives of state variables. Above all, proxy-based sliding mode control PSMC has brought the attention of most researchers for its simplicity of control architecture. It integrates the features of the PID controller and sliding mode control with ensured continuous closed-loop dynamics. In the PSMC, the signum function is rolled out to a saturated function without any approximation and hence the closed-loop dynamics have continuous behaviour. PSMC is applied to soft robotics for its superiority to ensure safety and precision in motion [38-43]. However, the stability of PSMC is not well treated and further work is required. Thus, the key point of this work is that it integrates three control units (PID+SMC+AAC) to obtain high control performance. First, it reformulates the structure of the PID controller integrating the features of the robust sliding mode control. Secondly, an adaptive approximation compensator is added to the control architecture to compensate for modelling errors if exist.

In view of the above, this paper deals with modelling and PMSC with an AAC term for flexible beams with piezo-patches. The role of AAC is to compensating for unmodelled dynamics and to ease the task of proof of system stability. Whereas the PMSC unit attempts to capture the features of the PID control and the SMC with continuous closed-loop dynamics. The Euler-Bernoulli beam theory is used for derivation of dynamics of the target smart beam. The partial differential equation PDF of the vibrating beam is transformed into second-order differential equations ODEs with definite mode shapes using the Galerkin method. A simply supported beam is simulated by MATLAB/SIMULINK package considering the first two-mode shapes. Two collocated piezo-patches are placed optimally on the vibrating beam working as actuators and sensors. Several experiments are performed to prove verification and precise regulation of PMSC.

The rest of the paper is organized as follows. Dynamic modelling of the Euler-Bernoulli beam and the proposed control structure are presented in Section 2. Section. Simulation experiments are introduced in Section 3 while Section 4 concludes.

2. METHODOLOGY

2.1 Dynamic modelling of smart beams

In general, there are three well-known beam theories for derivation of equation of motion: 1) Euler-Bernoulli theory that neglects rotational inertia and shear deformation and it is suitable for thin beams, 2) Rayleigh theory in which shear deformation is considered, and 3) Timoshenko beam that considers both rotational inertia and shear deformation and it is suitable for thick beams [8]. This paper is focused on Euler-Bernoulli beam theory in the modelling of flexible beams. In Figure 1, a thin prismatic beam with constant flexural rigidity $E_b I_b$. It is excited by a distributed force f (x, t) over the length of the beam and provided with surface bonded piezo-patches. The dimension of the beam and piezo-patches are shown in the figure. The following assumptions are proposed for modelling of the target beam.

Assumption 1. The beam is thin enough that Euler beam theory is applied.

Assumption 2. The stiffness and inertia of the piezo-patches are neglected.

Assumption 3. Sufficient transducers (or piezo-sensors) are available such that modal amplitudes are measurable.

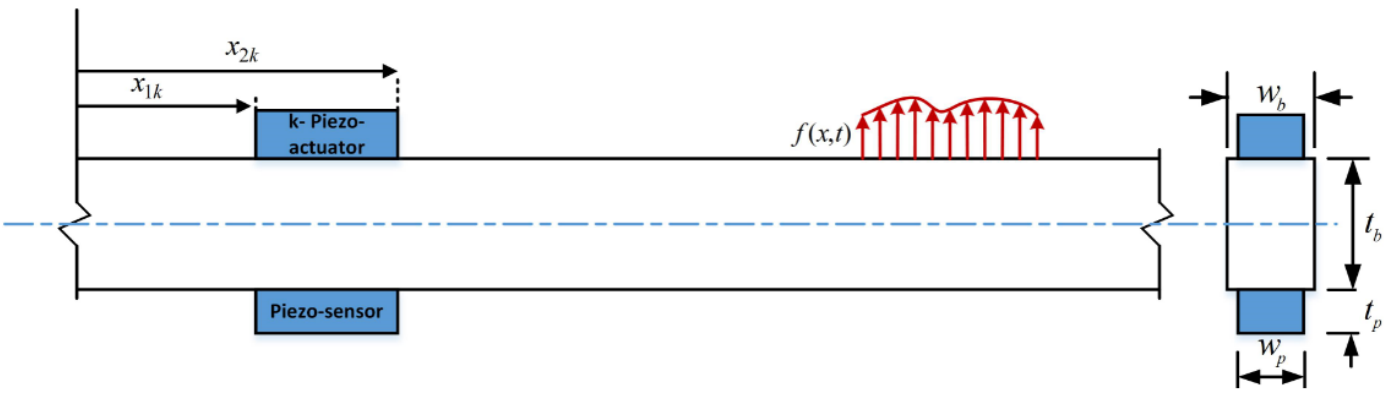

Figure 1. A flexible beam with piezo-patches

Remark 1. In effect, all three assumptions mentioned above are reasonable and necessary for our current work. In Assumption 1, the beam is considered thin such that we can apply Euler-Bernoulli beam theory. If the beam is considered thick then we should depend on Timoshenko beam theory for modelling purpose [8]. For Assumption 2, the dynamics of the piezo-transducers are neglected since the vibration characteristics of the vibrating beam would not be affected by the attached piezo-transducers [44]. Assumption 3 means that the modal amplitudes can be observed (measured) depending on installing a sufficient number of sensors [7].

The governing PDF for the transverse bending deflection y of Euler-Bernoulli beams can be expressed as [7, 45]:

$$E_b I_b \frac{\partial^4 y(x,t)}{\partial x^4} + c\frac{\partial y}{\partial t} + \rho_b A_b \frac{\partial^2 y(x,t)}{\partial t^2} = f(x,t) - \frac{\partial^2 M_p(t)}{\partial x^2} \tag{1}$$

where, E_b, I_b, ρ_b, A_b and c are modulus of elasticity, moment of inertia, density, cross-sectional area of the beam, and damping coefficient respectively. $M_p\ (x,\ t)$ represents the applied bending moment exerted by a piezo-actuator and it can be expressed as [7]:

$$M_p(x,t) = Dv_a(t)[H(x-x_1) - H(x-x_2)] \tag{2}$$

where, $v_a(t)$ is an excitation voltage applied to the piezo-actuator. The constant D depends on the dimensions and material properties of both beam and piezo-actuator [13], $x_{(.)}$ refers to the location of piezo-actuator, and H(.) is a Heaviside step function. Using Galerkin method, the transverse displacement of the target beam can be approximated as:

$$y(x,t) \cong \sum_{i=1}^{N} \phi_i(x) q_i(t) \qquad i = 1,2,3,\cdots N \tag{3}$$

where, $q_i(t)$ is a time dependent function (modal amplitudes), N refers to the number of mode shapes, and $\phi_i(x)$ is the mode shape of the beam. Thus, Eq. (1) can be expressed as:

$$\begin{aligned} E_b I_b \sum_{j=1}^{N} \phi_j''''(x)\, q_j(t) + c\sum_{j=1}^{N} \phi_j(x)\dot{q}_j(t) \\ + \rho_b A_b \sum_{j=1}^{N} \phi_j(x)\ddot{q}_j(t) \\ = f(x,t) - Dv_a(t)\frac{\partial^2}{\partial x^2}[H(x-x_1) \\ - H(x-x_2)] \end{aligned} \tag{4}$$

Multiplying Eq. (4) by $\phi_i(x)$, $(i \neq j)$ and integrating over the length of the beam to obtain the following decoupled system.

$$\begin{aligned} E_b I_b \int_0^{l_b} \phi_i''''(x)\phi_i(x)\,dx\, q_j(t) \\ + c\int_0^{l_b} \phi_i(x)\phi_i(x)dx\, \dot{q}_j(t) \\ + \rho_b A_b \int_0^{l_b} \phi_i(x)\phi_i(x)dx\, \ddot{q}_j(t) \\ = \int_0^{l_b} f(x,t)\phi_i(x)dx \\ - \int_0^{l_b} Dv_a(t)\phi_i(x)\frac{\partial^2}{\partial x^2}[H(x-x_1) \\ - H(x-x_2)]\,dx \end{aligned} \tag{5}$$

Eq. (5) can systematically be expressed as:

$$\begin{aligned} m_i\ddot{q}_i(t) + c_i\dot{q}_i(t) + k_i q_i(t) = g_i(x,t) - \mu_i v_a(t), \\ i = 1,2,3,\dots,N \end{aligned} \tag{6}$$

with

$$\begin{aligned} m_i &= \rho_b A_b \int_0^{l_b} \phi_i(x)\phi_i(x)dx, \\ c_i &= c\int_0^{l_b} \phi_i(x)\phi_i(x)dx, \\ k_i &= E_b I_b \int_0^{l_b} \phi_i''''(x)\phi_i(x)\,dx, \\ w_{ni}^2 &= \frac{k_i}{m_i}, \\ g_i(t) &= \int_0^{l_b} f(x,t)\phi_i(x)dx, \\ \mu_i &= D(\phi_i'(x_2) - \phi_i'(x_1)) \end{aligned} \tag{7}$$

However, there are N_a piezo-actuators bonded on the beam and hence by using superposition technique, Eq. (6) can be rewritten as:

$$\begin{aligned} m_i\ddot{q}_i(t) + c_i\dot{q}_i(t) + k_i q_i(t) \\ = g_i(x,t) - \sum_{k=1}^{N_a} \mu_{ik} v_{ak}(t) \\ , i = 1,2,3,\dots,N \end{aligned} \tag{8}$$

with N_a being the number of piezo-actuators and μ_{ik} being defined in Eq. (7) with modification of subscripts for x_1 and x_2 to x_{1k} and x_{2k} respectively to distinguish locations of multi-piezo-actuators, where k=1,2,3…N_a.

Eq. (8) can extend for multi-modal analysis using matrix representation to get,

$$M\ddot{q} + C\dot{q} + Kq + g = u \tag{9}$$

where,

$$\begin{aligned} \mathrm{M} = \begin{pmatrix} m_1 & \cdots & 0 \\ \vdots & \ddots & \vdots \\ 0 & \cdots & m_N \end{pmatrix} \in R^{N\times N}, C = \begin{pmatrix} c_1 & \cdots & 0 \\ \vdots & \ddots & \vdots \\ 0 & \cdots & c_N \end{pmatrix} \in R^{N\times N}, \\ K = \begin{pmatrix} k_1 & \cdots & 0 \\ \vdots & \ddots & \vdots \\ 0 & \cdots & k_N \end{pmatrix} \in R^{N\times N}, g = \begin{pmatrix} -g_1 \\ \vdots \\ -g_N \end{pmatrix} \in R^N, \\ \mu = \begin{pmatrix} -\mu_{11} & \cdots & -\mu_{1NN_a} \\ \vdots & \ddots & \vdots \\ -\mu_{N1} & \cdots & -\mu_{NN_a} \end{pmatrix} R^{N\times N_a}, u = \mu v_a \in R^N \end{aligned}$$

Eq. (9) is similar to multi-degrees-of-freedom 2nd-order discrete dynamic systems. The following points should be noted:

I. The matrices M, C and K are diagonal matrices and hence the dynamic system is decoupled on the left-side of Eq. (9). However, the coupling interaction at the input coefficient μ for multi-modal dynamics.

II. The matrix M has constant-value elements (assuming beams with constant cross-section) while C is assumed a positive definite matrix.

III. The state variable q cannot be sensed (measured) directly, its reading depends on sensor voltage readings.

In the following, we will attempt to reformulate Eq. (9) such that the output state variables are piezo-sensor voltages v_s. Thus, v_s can be represented as [7]:

$$v_{sj} = \sum_{k=1}^{N} \alpha_{jk} q_k(t) = [\alpha_{j1} \quad \dots \quad \alpha_{jN}] \begin{bmatrix} q_1 \\ \vdots \\ q_N \end{bmatrix}, \quad j = 1,2,3,\dots,N_s \tag{10}$$

where, $\alpha_{(.)}$ is a constant that depends on the location of piezo-sensors and N_s is the number of piezo-sensors that are equal to N_a in case of collocated patches. In matrix/vector representation, Eq. (10) can be rewritten as:

$$\mathrm{v_s} = \alpha\, q, \quad \alpha = \begin{pmatrix} \alpha_{11} & \cdots & \alpha_{1N} \\ \vdots & \ddots & \vdots \\ \alpha_{N_s 1} & \cdots & \alpha_{N_s N} \end{pmatrix} \in R^{N_s \times N} \tag{11}$$

Therefore, substituting Eq. (11) into Eq. (9) results in

$$M\alpha^{+}\ddot{\mathrm{v}}_s + C\alpha^{+}\dot{\mathrm{v}}_s + K\alpha^{+}\mathrm{v}_s + g = u \tag{12}$$

where, $\alpha^{+} \in R^{N \times N_s}$ is the Moore-Penrose inverse matrix of sensor gain matrix (α), see the paper [46] for more details.

2.2 Control structure

This subsection deals with integration of the PSMC and the AAC for vibration suppression of smart beams. The PSMC was well applied to different applications especially soft robotics. It is an improved and continuous version of sliding mode control that integrates the features of PID control family and the robust sliding mode control. The key idea of this strategy is to impose a null virtual mass called a proxy in between PID controller on the side of output target system (the dynamic system that is required to be controlled) and a sliding mode control on the end of the virtual proxy object. It attempts to control (regulate) local and global dynamics associated with the PID control and the SMC respectively [38]. As a result, the PSMC has superior features of accurate tracking and safe recovery while the disturbed system is under external disturbances.

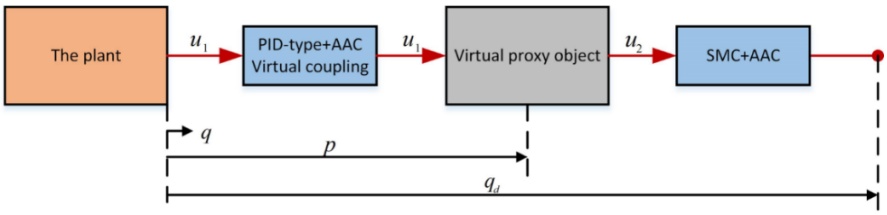

Figure 2. A simplified sketch showing the concept of the PSMC

Figure 2 describes concept of PSMC for the target smart system (equivalent system according to Eq. (9)). The stability of the PSMC is not well addressed. Besides, most previous work was focused on proving that the closed loop dynamics is passive in order to compensate for disturbances if exist. To this end, this section proposes the PSMC combined with an adaptive approximation term to compensate for disturbances if exist. This technique simplifies proof of stability of the dynamic system and makes the derivation straightforward.

According to the principle of PSMC described in Figure 2, consider the following position errors and sliding surfaces:

$$e = q_d - q,\ \sigma = (q_d - q) + \Lambda(\dot{q}_d - \dot{q}) = e + \Lambda\dot{e} \tag{13a}$$

$$e_\chi = \chi - q,$$
$$\sigma_\chi = (\chi - q) + \Lambda(\dot{\chi} - \dot{q}) = e_\chi + \Lambda\dot{e}_\chi \tag{13b}$$

$$e_s = q_d - \chi,$$
$$\sigma_s = (q_d - \chi) + \Lambda(\dot{q}_d - \dot{\chi}) = e_s + \Lambda\dot{e}_s \tag{13c}$$

where, e, e_x and $e_s \in \mathrm{R^N}$ are actual position error, position error associated with PD, and position error associated with sliding mode control respectively with corresponding sliding surfaces σ, σ_χ and $\sigma_s \in \mathrm{R^N}$. $q_d \in \mathrm{R^N}$ is the desired trajectory, $\chi \in \mathrm{R^N}$ is the proxy position while $\Lambda \in \mathrm{R^{N\times N}}$ is a diagonal positive definite feedback gain matrix. According to Figure 2, the intuitive control law for can be designed as:

$$u = u_1 = \underbrace{\hat{\xi}}_{AAC} + \underbrace{K_\chi e_\chi + K_d \dot{e}_\chi}_{PD} \tag{14a}$$

with

$$\hat{\xi} = \hat{M}\ddot{q}_d + \hat{C}\dot{q}_d + \hat{K}q_d + \hat{g} = \hat{M}\ddot{q}_d + \hat{C}\dot{q}_d + \hat{\eta},$$

$$\hat{\eta} = \hat{K}q_d + \hat{g}$$

where, $\hat{\xi} \in \mathrm{R^N}$ is a lumped uncertain vector that can be approximated by a linear combination of orthogonal functions, and the symbol $\hat{(.)}$ refers to estimation. Thus, the estimated term $\hat{\xi}$ can be expressed as:

$$\hat{\xi} = \hat{W}^T\varphi \tag{14b}$$

where, $\hat{W} \in \mathrm{R^{N\beta\times N}}$ is the weighting coefficient matrix that should be updated and $\varphi \in \mathrm{R^{N\beta}}$ is the orthogonal basis vector, with β referring to the number of basis function terms. The following update law is selected with ensured stability:

$$\dot{\hat{W}} = Q^{-1}\varphi\dot{e}^T \tag{14c}$$

where, $Q \in \mathrm{R^{N\beta\times N\beta}}$ a diagonal positive-definite adaptation gain matrix. Now the role of PSMC comes. Using the principle of proxy-based sliding mode control (see Figure 2) with modification of original version proposed by Kikuuwe et al. [37], the dynamics of proxy can be modelled as

$$m_\chi\ddot{\chi} = 0 = u_1 - u_2 \tag{15}$$

with $m_\chi \in \mathrm{R^{N\times N}}$ being the virtual proxy mass, and

$$u_2 = \hat{\xi} + Usgn(\sigma_s) \tag{16}$$

where, $\mathrm{U} \in \mathrm{R^N}$ is constant coefficient vector that limits the values of control input. Alternatively, Eq. (15) can be expressed as:

$$\hat{\xi} + K_\chi e_\chi + K_d \dot{e}_\chi = \hat{\xi} + Usgn(\sigma_s) \tag{17}$$

Eq. (17) can be rewritten as:

$$K_\chi e_\chi + K_d \dot{e}_\chi = Usgn(\psi - \Lambda \dot{e}_\chi) \tag{18}$$

with $\psi = \sigma - e_\chi$. Using the following mathematical expression [37, 38],

$$\begin{aligned} a_1 &= a_2 + a_3 sgn(a_4 - a_5 a_1) \\ &= a_2 + a_3 sat\left(\frac{a_4}{a_5 a_3} - \frac{a_2}{a_3}\right) \end{aligned} \tag{19}$$

According to the above equation, Eq. (18) can be reformulated as:

$$\begin{aligned} \dot{e}_\chi = -K_d^{-1} K_\chi e_\chi + K_d^{-1} Usat(U^{-1} K_d\ \Lambda^{-1}\psi \\ + U^{-1} K_\chi e_\chi) \end{aligned} \tag{20}$$

Thus, the desired control voltage presented in Eq. (14a) can be designed as:

$$u = u_1 = \hat{\xi} + Usat(U^{-1} K_d\ \Lambda^{-1}\psi + U^{-1} K_\chi e_\chi) \tag{21}$$

Equating Eq. (9) to Eq. (14a) leads to the following closed-loop dynamics,

$$\begin{aligned} M\ddot{q} + C\dot{q} + \underbrace{Kq + g}_{\eta} = \hat{M}\ddot{q}_d + \hat{C}\dot{q}_d + \underbrace{\hat{K}q_d + \hat{g}}_{\hat{\eta}} + \\ K_\chi e_\chi + K_d \dot{e}_\chi \end{aligned} \tag{22}$$

By adding $(-M\ddot{q}_d - C\dot{q}_d - \eta)$ to both sides of above equation to obtain,

$$-M\ddot{e} - C\dot{e} = \tilde{M}\ddot{q}_d + \tilde{C}\dot{q}_d + \tilde{\eta} + K_\chi e_\chi + K_d \dot{e}_\chi + \epsilon \tag{23}$$

with $\tilde{(.)} - (.) = \tilde{(.)}$. Eq. (23) can be represented as:

$$\begin{aligned} M\ddot{e} + C\dot{e} &= -\tilde{\xi} - K_\chi e_\chi - K_d \dot{e}_\chi + \epsilon \\ &= -\tilde{W}^T \varphi - K_\chi e_\chi - K_d \dot{e}_\chi + \epsilon \end{aligned} \tag{24}$$

where, $\epsilon \in \mathrm{R}^N$ is the approximation modelling error.

Theorem. The dynamics of the target smart beam modelled in Eq. (9) with the control law presented in Eq. (21), the adaptive law of Eq. (14c), and the closed-loop dynamics given in Eq. (24) is stable in the sense of Lyapunov theory.

Proof.

Consider the following Lyapunov-like candidate along the trajectory of Eq. (24)

$$\begin{aligned} V = \frac{1}{2}\dot{e}^T M \dot{e} + \frac{1}{2} tr\left(\tilde{W}^T Q \tilde{W}\right) + \frac{1}{2} e_\chi^T K_\chi e_\chi \\ + \|U e_s\|_1 \end{aligned} \tag{25}$$

Taking derivative of above equation and substituting Eq. (23) into Eq. (25) to get,

$$\begin{aligned} \dot{V} = \dot{e}^T\left(-C\dot{e} - \tilde{W}^T\varphi - K_\chi e_\chi - K_d \dot{e}_\chi + \epsilon\right) \\ + tr\left(\tilde{W}^T Q \dot{\hat{W}}\right) + \dot{e}_\chi^T K_\chi e_\chi \\ + \dot{e}_s Usgn(e_s) \end{aligned} \tag{26}$$

Substituting Eq. (17) into above equation to obtain,

$$\begin{aligned} \dot{V} = -\dot{e}^T C\dot{e} + \dot{e}^T\epsilon + tr\left(\tilde{W}^T\left(-\varphi\dot{e}^T + Q\dot{\hat{W}}\right)\right) \\ - \dot{e}^T Usgn(\sigma_s) + \dot{e}_\chi^T(Usgn(\sigma_s) \\ - K_d\dot{e}_\chi) + \dot{e}_s Usgn(e_s) \end{aligned} \tag{27}$$

Applying Eq. (14c) keeping in mind that $C \geq 0$, then the above equation is reduced to,

$$\begin{aligned} \dot{V} = -\dot{e}^T C\dot{e} + \dot{e}^T\epsilon - \dot{e}_\chi^T K_d \dot{e}_\chi - \dot{e}^T Usgn(\sigma_s) \\ + \dot{e}_\chi^T Usgn(\sigma_s) + \dot{e}_s Usgn(e_s) \end{aligned} \tag{28}$$

From Eq. (13), we can get,

$$\dot{e}_\chi + \dot{e}_s = \dot{e} \tag{29}$$

Substituting Eqns. (29) and (13c) into Eq. (28) leads to,

$$\begin{aligned} \dot{V} = -\dot{e}^T C\dot{e} + \dot{e}^T\epsilon - \dot{e}_\chi^T K_d \dot{e}_\chi \\ - \dot{e}_s^T Usgn(e_s + \Lambda\dot{e}_s) \\ + \dot{e}_s^T Usgn(e_s) \end{aligned} \tag{30}$$

Using the following mathematical inequality,

$$y^T U[sgn(z + y) - sgn(z)] \geq 0 \tag{31}$$

Therefore, Eq. (30) is reduced to:

$$\dot{V} \leq -\dot{e}^T C\dot{e} - \dot{e}_\chi^T K_d \dot{e}_\chi + \dot{e}^T\epsilon \tag{32a}$$

Now let us deal with the last term exploiting the following inequality [47]:

$$\dot{e}^T\epsilon \leq \dot{e}^T\Omega^{-1}\dot{e} + \epsilon^T\Omega\epsilon \leq \dot{e}^T\Omega^{-1}\dot{e} + \bar{\epsilon} \tag{32b}$$

Thus, Eq. (32a) becomes,

$$\dot{V} \leq -\dot{e}^T C\dot{e} - \dot{e}_\chi^T K_d \dot{e}_\chi + \dot{e}^T\Omega^{-1}\dot{e} + \bar{\epsilon} \tag{32c}$$

where $\bar{\epsilon}$ is the upper bound of $\boldsymbol{\epsilon}$ such that $\epsilon^T\Omega\epsilon \leq \bar{\epsilon}$. To ensure stability, it is necessary to have $(C \geq \Omega^{-1})$ then the tracking error is bounded and converges to $\bar{\epsilon}$. Thus, the system is stable in sense of Lyapunov stability [23-28].

Remark 2. The above-mentioned stability proof requires knowledge of lower bounds of the damping matrix **C**. Other robust approaches are possible to avoid this choice such as dead-zone technique, see, e.g. [48] for more details.

3. SIMULATION RESULTS AND DISCUSSIONS

This section deals with simulation of a simply supported beam depicting in Figure 3. The physical parameters of the investigated smart beam are given in Tables 1 and 2. Two collocated piezo-patches are bonded to the surface of the beam for suppression of the resulted vibration. The dynamics of piezo-patches are neglected in comparison with the regular beam dynamics, see the paper [44] for more details. In effect, considering dynamics of piezo-patches would complicate the control problem since the equation of motion for the overall system is no longer decoupled and advanced control strategies are required.

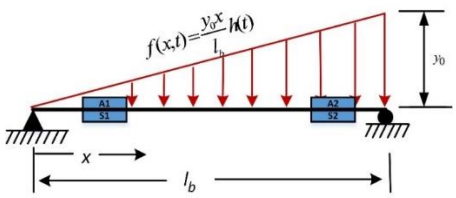

Figure 3. A flexible simply supported beam with the surface-bonded piezo-patches. The symbols A and S refer to piezo-actuator and sensor respectively. The function h(t) can be impulse or sinusoidal force

Table 1. Parameters of the beam

Property	Value
Density, ρ_b	8030 kg/m^3
Young's modulus, E_b	193×10^9pa
Length, l_b	0.3 m
Section width, w_b	0.03 m
Section thickness, t_b	$0.5\times10^{-3}m$
Damping coefficients	$c_1 = 00068\ N.\frac{s}{m}$ $c_2 = 0.028\ N.\frac{s}{m}$

Table 2. Parameters of the piezo-patches*

Property	Value
Young's modulus, E_p	68×10^9Pa
Length, l_p	0.075m
Section width, w_p	0.025m
Section thickness, t_p	$0.35\times10^{-3}m$
Location of 1st piezo, x_{11}, x_{21}	$x_{11} = 0.3(l_b) - \frac{l_p}{2}$, $x_{21} = 0.3(l_b) + \frac{l_p}{2}$
Location of 2nd piezo, x_{12}, x_{22}	$x_{12} = 0.7(l_b) - \frac{l_p}{2}$, $x_{22} = 0.7(l_b) + \frac{l_p}{2}$

*For detailed formulae used for evaluation of values of D and $\alpha_{(.)}$, see ref. [8].

Below, we will describe the mode shapes and frequency response for the first two modes shapes neglecting high order mode shapes. Then, a detailed comparison study is implemented including three scenarios. Scenario 1 includes disturbing the smart beam while no feedback loop is established (open-loop system). In scenario 2, a PD controller is applied on the vibrating beam to attenuate the produced vibration due to the excitation disturbance force. Whereas, scenario 3 includes application of the proposed control structure (PSMC+AAC) for vibration suppression of the flexible beam. For all previously mentioned scenarios, two types of disturbances are investigated separately: 1) an impulse force of 1 N peak and 1 s pulse width, and 2) sinusoidal disturbance with 0.5 N amplitude and 20 Hz frequency.

3.1 Frequency response and mode shapes

This subsection is focused on frequency response for the vibrating simply supported beam considering multi-piezo-patches. The piezo-patches are located where large sensor voltage readings are obtained. To capture the transfer functions for multi-input multi-output systems, let us recall Eq. (12a) with null excitation force, g=0.

$$\alpha^+ M\ddot{v}_s + \alpha^+ C\dot{v}_s + \alpha^+ Kv_s = u \tag{33}$$

Multiplying Eq. (33) by α, taking Laplace transform, and substituting $u = \mu v_a$, it becomes:

$$\frac{V_s(s)}{V_a(s)} = \alpha(Ms^2 + Cs + Ks)^{-1}\,\mu \tag{34}$$

Fortunately, $N_a = N_s = 2$, hence four transfer functions are obtained,

$$\frac{V_s(s)}{V_a(s)} = \begin{bmatrix} g_{11} & g_{12} \\ g_{21} & g_{22} \end{bmatrix} \tag{35}$$

Eq. (34) can be reformulated to represent the output in terms of the modal amplitudes as follows. Since $V_s(s) = \alpha\, Q(s)$, hence Eq. (34) becomes,

$$\frac{Q(s)}{V_a(s)} = (Ms^2 + Cs + Ks)^{-1}\mu \tag{36}$$

However, it is realistic to deal with the total deflection of the plate as an output. By recalling Eq. (8), the following transfer function is obtained,

$$G(x,s) = \sum_{i=1}^{N} \frac{\phi_i(x)}{m_i s^2 + c_i s + k_i s}[\mu_{i1} \quad \dots \quad \mu_{iNa}] \tag{37}$$

Eq. (37) is used as a basis for determination of frequency response of the vibrating beam considering multi-piezo-patches with multi-mode shapes. Here the deflection frequency response depends on the basis function $\phi_i(x)$ that is a function of the displacement x. Besides, the first two mode shapes in the low-frequency region are considered since they have larger amplitudes in comparison to high-frequency amplitudes.

3.2 Impulse disturbance

Now consider the simply supported beam described in Figure 3. The target beam is subjected to an impulse force with 10 N peak and 2 s pulse width. Three experiments are implemented to investigate the validity of the proposed controller. In experiment 1, the target beam is vibrated under the impulse force without using a feedback control (open-loop system). Experiment 2 includes implementation of the PD controller on the target-vibrating beam while in experiment 3, the proposed PSMC+AAC is performed. The feedback gains used in experiment 2 are: $K_p = 400I_2, K_d = 100I_2$, where I_i is $i\times i$ identity matrix. Whereas, for experiment 3, the following feedback and adaptation gains are used in simulation: $\Lambda = 20I_2, K_p = 400I_2, K_d = 100I_2, U = I_2, Q = 75I_{22}$.

According to Eq. (8), the i-mode equation of motion for the simply supported beam can be expressed as:

$$m_i\ddot{q}_i(t) + c_i\dot{q}_i + k_i q_i(t) = \sum_{k=1}^{N_a} \mu_{ik} v_{ak}(t) - g_i(x,t) \tag{38}$$

$$, i = 1,2.$$

with m_i, c_i, k_i being defined in Eq. (6), $N = N_a = N_s = 2$ such that the actuator and sensor gain matrices are square that

can facilitate the task of controller, and the exciting force is selected as:

$$g_i(x,t) = \int_0^{l_b} f(x,t)\phi_i(x)dx = h(t)\int_0^{l_b} \frac{y_0 x}{l_b} sin\frac{i\pi x}{l_b} dx = -\frac{l_b y_0}{i\pi} h(t)(-1)^i, i = 1,2 \quad (39)$$

where, y_0=1 and h(t) are the excitation impulse force. The objective of the controller is to attenuate (suppress) the vibration resulted due to the applied impulse force. The proposed control law described in Eq. (21) with the update adaptive law presented in Eq. (14c) is implemented using MATLAB/SIMULINK package. As aforementioned, the control law consists of two terms: a PSMC term plus an AAC term for compensation purposes. Orthogonal Chebyshev polynomials with β=15 is used as approximators. In the tuning process, the gains are gradually increased from zero to a value at which the system is oscillating then the gain values are halved. The output amplitude displacements are depicted in Figure 4 while the control input is plotted in Figure 5. As seen in the plots, it can be concluded that the proposed control architecture damps out the resulted vibration with high performance in comparison with conventional PD. In addition, if the number of piezo-patches are not equal to the number of mode shapes, then a pseudo-inverse matrix is a powerful tool to determine the input voltages.

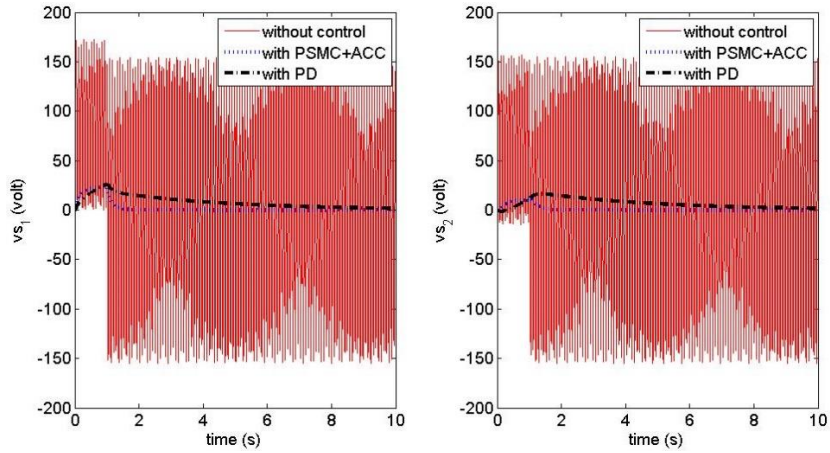

Figure 4. The modal displacement response-impulse disturbance signal

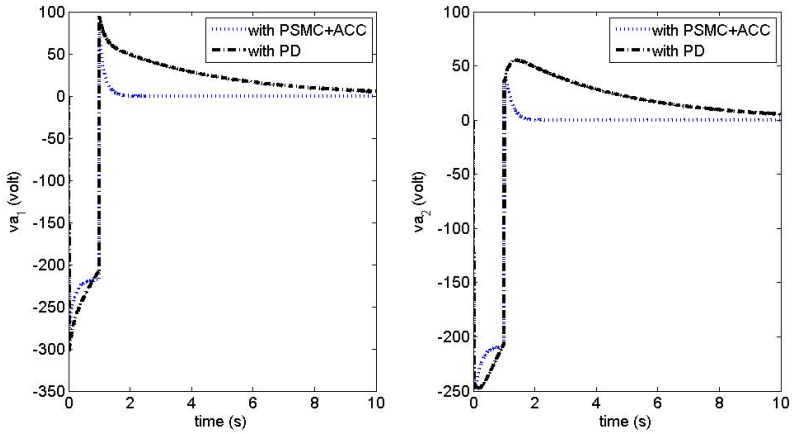

Figure 5. The control input voltages-impulse disturbance signal

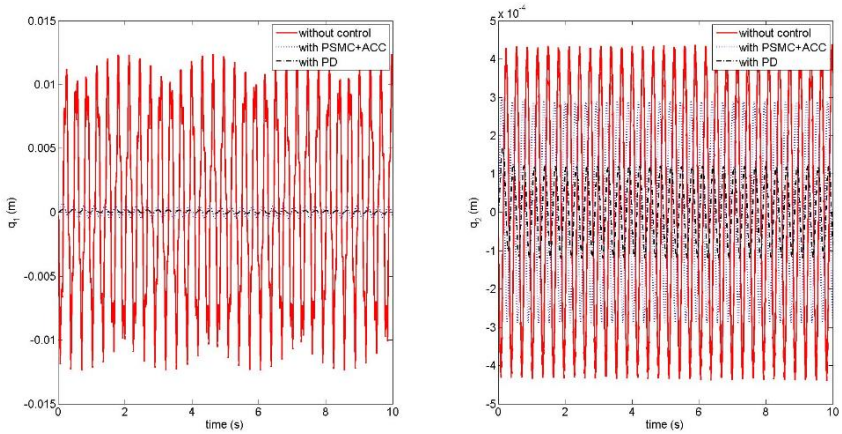

Figure 6. The modal displacement response-sinusoidal disturbance signal

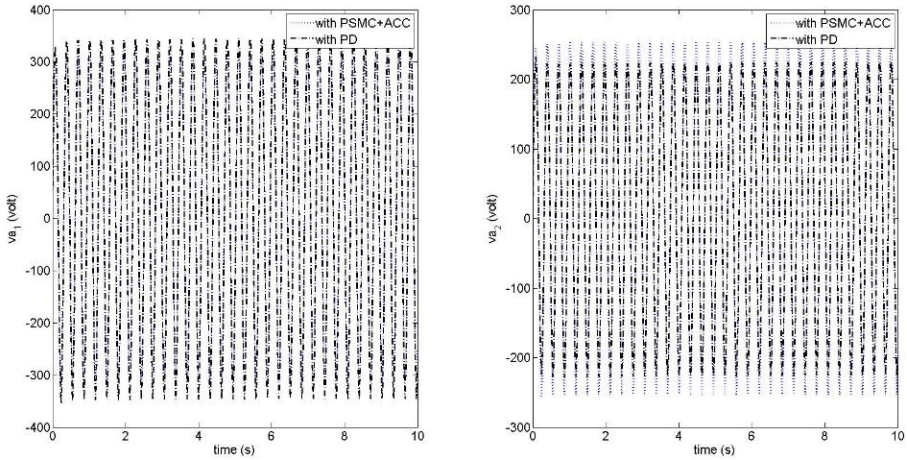

Figure 7. The control input voltages-sinusoidal disturbance signal

3.3 Sinusoidal disturbance

In a similar manner to Sec. 3.2, three experiments are performed including the open-loop system, the PD controller, and the PSMC+AAC respectively. This section differs from the previous sub-section in the type of disturbance signal used. A sinusoidal

Excitation force with 0.5 N amplitude and 20 Hz frequency is used for all three experiments. In experiment 1, the vibrating smart beam is disturbed without application of any feedback loop (open-loop system) and hence the beam system will vibrate freely. Whereas, in experiments 2 and 3 a PD controller and a PSMC+AAC are applied separately and respectively on the vibrating beam under a harmonic excited force. The same feedback gains mentioned for Sec. 3.2 are used here. In addition, Chebyshev polynomials with β=15 are used as approximators for adaptive scheme. As expected, the PSMC+AAC works well in vibration suppression of the vibrating beam. The modal responses for the first two mode shapes are depicted in Figure 6 while the response of the input control is described in Figure 7. It should be noted that both the PD and the PSMC work well in a sinusoidal disturbance signal and there could be no superiority for the PSMC in the case of a harmonic sinusoidal disturbance.

4. CONCLUSIONS

This paper is concerned with a modified version of the PSMC by adding AAC term for vibration control of Euler-Bernoulli beam. The key idea of the PSMC is to combine the features of the PID and the SMC. Whereas, the AAC includes representation of the uncertainty in terms of a weighting coefficient and basis function matrices/vectors. The performance and stability of the proposed control structure is approved using Lyapunov theory. The dynamics of vibrating beam with the attached piezo-patches are derived systematically in standard 2nd order differential equations considering definite mode shapes. Despite the current work does not consider a nonlinear model for the smart beam, it can be straightforward used for complex dynamics of smart beams with miscellaneous disturbance signals since the control structure includes a robust feedback term represented by the PSMC and a feedforward term denoted by the adaptive approximation compensator. Future works are required to deal with the following issues:

(1) Spillover phenomenon resulted from the effect of vibration of unmodelled mode shapes.

(2) The nonlinear dynamics are not modelled in the current work; however, our proposed control is a promising control scheme for nonlinear beam models.

(3) Vibration suppression of large-scale flexible structures such as plates and shells.

(4) Considering dynamics of the piezo-transducers in beam modelling. This can complicate the control problem since the mode shapes are coupled in this case.

REFERENCES

[1] Hu, Q.L. (2009). A composite control scheme for attitude maneuvering and elastic mode stabilization of flexible spacecraft with measurable output feedback. Journal of Aerospace Science and Technology, 13(2-3): 81-91. https://doi.org/10.1016/j.ast.2007.06.007

[2] Suleman, A., Costa, A.P. (2004). Adaptive control of an aeroelastic flight vehicle using piezoelectric actuators. Journal of Computers & Structures, 82(17-19): 1303-1314. https://doi.org/10.1016/j.compstruc.2004.03.027

[3] Liu, L.K., Zheng, G.T. (2007). Parameter analysis of PAF for a whole-spacecraft vibration isolation. Journal of Aerospace Science and Technology, 11(6): 464-472. https://doi.org/10.1016/j.ast.2007.02.006

[4] García, B., Burgos, J.C., Alonso, Á. (2005). Winding deformations detection in power transformers by tank vibrations monitoring. Journal of Electric Power Systems Research, 74(1): 129-138. https://doi.org/10.1016/j.epsr.2004.09.010

[5] Kircali, Ö.F. (2006). Active vibration control of a smart beam: a spatial approach. MSc Thesis, Graduate School of Natural and Applied Sciences, Middle East Technical University, Turkey.

[6] Bandyopadhyay, B., Manjunath, T.C., Umapathy, M. (2007). Modeling, Control and Implementation of Smart Structures: A FEM-State Space Approach. Springer-Verlag Berlin Heidelberg.

[7] Wagg, D., Neild, S. (2010). Nonlinear Vibration with Control. Springer, Cham. https://doi.org/10.1007/978-3-319-10644-1

[8] Rao, S.S. (2007). Vibration of Continuous Systems. John Wiley and Sons, Inc.

[9] Weldegiorgis, R., Krishna, P., Gangadharan, K.V. (2014).

Vibration control of smart cantilever beam using strain rate feedback. Procedia Materials Science, 5: 113-122. https://doi.org/10.1016/j.mspro.2014.07.248

[10] Omidi, E., Mahmoodi, S.N., Shepard, W.S. (2016). Multi positive feedback control method for active vibration suppression in flexible structures. Mechatronics, 33: 23-33. https://doi.org/10.1016/j.mechatronics.2015.12.003

[11] Song, G., Agrawal, N.B. (2001). Vibration suppression of flexible spacecraft during attitude control. Acta Astronautica, 49: 73-83. https://doi.org/10.1016/S0094-5765(00)00163-6

[12] Zhang, S., Schmidt, R., Qin, X. (2015). Active vibration control of piezoelectric bonded smart structures using PID algorithm. Chinese Journal of Aeronautics, 28: 305-313. https://doi.org/10.1016/j.cja.2014.12.005

[13] Le, S. (2009). Active Vibration Control of a Flexible Beam. Master thesis, San Jose State University, USA.

[14] Jovanova, J., Gvriloski, V., Djidrov, M., Tasevsk G. (2015). Model based vibration control of smart flexible structure using piezoelectric transducers. FME Transactions, 43: 70-75. https://doi.org/10.5937/fmet1501070J

[15] Wang, X., Gao, Z., Fang, Y., Hu , J., Zhu , X. (2019). Active vibration control of smart flexible piezoelectric beam with a tip mass using hybrid FX-VSSLMS algorithm. The Journal of Engineering, 2019(13): 172-174. https://doi.org/10.1049/joe.2018.9033

[16] Özer, A.Ö. (2017). Modeling and controlling an active constrained layer (ACL) beam actuated by two voltage sources with/without magnetic effects. IEEE Transactions on Automatic Control, 62(12): 6445-6450. https://doi.org/10.1109/TAC.2017.2653361

[17] Khot, S.M., Yelve, N.P., Kumar, P., Singh, D., Purohit, G.A. (2017). Simulation study of active vibration control of beams supported at both ends using optimal controllers. International Conference on Nascent Technologies in Engineering (ICNTE), Navi Mumbai, pp. 1-8. https://doi.org/10.1109/ICNTE.2017.7947894

[18] Da Silva, C.A.X., Colombo, D.A., Koroishi, E.H., Molina, F.A.L., Taketa, E., Faria, A.W. (2016). Comparative study of the active vibration control using LQR and H-infinity norm in a beam of composite material. 2016 12th IEEE International Conference on Industry Applications (INDUSCON), Curitiba, 2016, pp. 1-6. https://doi.org/10.1109/INDUSCON.2016.7874526

[19] Djokoto, S.S., Dragašius E., Jūrėnas, V., Agelin-Chaab, M. (2020). Controlling of vibrations in micro-cantilever beam using a layer of active electrorheological fluid support. IEEE Sensors Journal, 20(8): 4072-4079. https://doi.org/10.1109/JSEN.2019.2961380

[20] Muresan, C.I., Folea, S., Birs, I.R., Ionescu, C.M. (2017). Fractional order modeling and control of a smart beam. 2017 IEEE Conference on Control Technology and Applications (CCTA), Mauna Lani, HI, pp. 1517-1523. https://doi.org/10.1109 /CCTA. 2017. 8062672

[21] Zhu, W.H. (2010). Virtual Decomposition Control: Toward Hyper Degrees of Freedom Robots. Springer-Verlag Berlin Heidelberg.

[22] Abdeljaber, O., Avci, O., Inman D.J. (2016). Active vibration control of flexible cantilever plates using piezoelectric materials and artificial neural networks. Journal of Sound and Vibration, 363: 33-53. https://doi.org/10.1016/j.jsv.2015.10.029

[23] Al-Shuka, H.F.N., Song, R. (2019). Decentralized adaptive partitioned approximation control of high degrees-of-freedom robotic manipulators considering three actuator control modes. International Journal of Dynamics and Control, 7: 744-757. https://doi.org/10.1007/s40435-018-0482-3

[24] Lewis, F.L., Yesildirek, A., Liu, K. (1995). Neural net robot controller: Structure and stability proofs. Journal of Intelligent and Robotic Systems, 13: 1-23. https://doi.org/10.1007/BF01262965

[25] Lewis, F.L., Liu, K., Yesildirek, A. (1995). Neural net robot controller with guaranteed tracking performance. IEEE Transactions on Neural Networks, 6(3): 703-716. https://doi.org/10.1109/72.377975

[26] Lewis, F.L., Yesildirek, A., Liu, K. (1996). Multilayer neural net robot controller with guaranteed tracking performance. IEEE Transactions on Neural Networks, 7(2): 1-12. https://doi.org/10.1109/72.485674

[27] Liu, J. (2013). Radial Basis Function (RBF) Neural Network Control for Mechanical Systems: Design, Analysis and Matlab Simulation. Tsinghua University Press, Beijing and Springer-Verlag Berlin Heidelberg.

[28] Huang, A.C., Chien, M.C. (2010). Adaptive Control of Robot Manipulators: A Unified Regressor-Free Approach. World Scientific Publishing Company; Illustrated edition.

[29] Ge, S.S., Lee, T.H., Harris, C.J. (1998). Adaptive Neural Network Control of Robotic Manipulators, World Scientific Publishing Co., Inc. River Edge, NJ, USA.

[30] Al-Shuka, H.F.N., Corves, B., Zhu, W.H. (2013). Function approximation technique-based adaptive virtual decomposition control for a serial-chain manipulator. Cambridge Journals, 32(3): 375-399. https://doi.org/10.1017/S0263574713000775

[31] Al-Shuka, H.F.N. (2018). On local approximation-based adaptive control with applications to robotic manipulators and biped robots. International Journal of Dynamics and Control, 6: 339-353. https://doi.org/10.1007/s40435-016-0302-6

[32] Al-Shuka, H.F.N., Song, R. (2018). Hybrid regressor and approximation-based adaptive control of piezoelectric flexible beams. 2018 2nd IEEE Advanced Information Management, Communicates, Electronic and Automation Control Conference (IMCEC), Xi'an, pp. 330-334. https://doi.org/10.1109/IMCEC.2018.8469279

[33] Al-Shuka, H.F.N., Song, R. (2018). Hybrid regressor and approximation-based adaptive control of robotic manipulators with contact-free motion. 2018 2nd IEEE Advanced Information Management, Communicates, Electronic and Automation Control Conference (IMCEC), Xi'an, pp. 325-329. https://doi.org/10.1109/IMCEC.2018.8469628

[34] Ding, G., Huang, J., Cao, Y. (2017). Proxy based sliding mode control for a class of second-order nonlinear system. In: Huang, Y., Wu, H., Liu, H., Yin, Z. (eds) Intelligent Robotics and Applications. ICIRA 2017. Lecture Notes in Computer Science, vol 10463. Springer, Cham. https://doi.org/10.1007/978-3-319-65292-4_76

[35] Slotine, J., Li, W. (1991). Applied Nonlinear Control. Prentice Hall, Upper Saddle River.

[36] Shtessel, Y., Edwards, C., Fridman, L., Levant, A. (2014). Sliding Mode Control and Observation. Springer.

[37] Kikuuwe, R., Yasukouchi, S., Fujitomo, H., Yamamoto, M. (2010) Proxy-based sliding mode control: A safer

extension of PID control. IEEE Trans. Robot, 26(4): 670-683. https://doi.org/10.1109/TRO.2010.2051188

[38] Kashiri, N., Tsagarakis, N.G., Van Damme, M., Vanderborght, B., Caldwell, D.G. (2016). Proxy-based sliding mode control of compliant joint manipulators. In: Filipe, J., Gusikhin, O., Madani, K., Sasiadek, J. (eds) Informatics in Control, Automation and Robotics. Lecture Notes in Electrical Engineering, vol 370. Springer, Cham. https://doi.org/10.1007/978-3-319-26453-0_14

[39] Kashiri, N., Lee, J., Tsagarakis, N.G., Van Damme, M., Vanderborght, B., Caldwell, D.G. (2016). Proxy-based position control of manipulators with passive compliant actuators: stability analysis and experiments. Robotics and Autonomous Systems, 75: 398-408. https://doi.org/10.1016/j.robot.2015.09.003

[40] Van Damme, M., Vanderborght, B., Verrelst, B., Van Ham, R., Daerden, F., Lefeber, D. (2009). Proxy-based sliding mode control of a planar pneumatic manipulator. The International Journal of Robotics Research, 28(2): 266-284. https://doi.org/10.1177/0278364908095842

[41] Ding, G., Huang, J., Hu, B., Guan, Z. (2017). Proxy-based sliding mode stabilization of a class of second-order nonlinear system. 2017 11th Asian Control Conference (ASCC), Gold Coast, QLD, pp. 2917-2922. https://doi.org/10.1109/ASCC.2017.8287641

[42] Wah, N., Aung, M.T.S. (2017). Proxy based sliding mode control augmented with friction compensator for use in 1-DOF freehand ultrasound probe. IECON 2017 - 43rd Annual Conference of the IEEE Industrial Electronics Society, Beijing, 2017, pp. 2911-2916. https://doi.org/10.1109/IECON.2017.8216491

[43] Gong, X., Sun, L., Liu, J. (2019). Proxy based sliding mode control for series elastic actuator based on algebraic identification and motion planning. Chinese Control and Decision Conference (CCDC), Nanchang, China, pp. 863-868. https://doi.org/10.1109/CCDC.2019.8832935

[44] Zhang, W., Meng, G., Li, H. (2006). Adaptive vibration control of micro-cantilever beam with piezoelectric actuator in MEMS. The International Journal of Advanced Manufacturing Technology, 28: 321-327. https://doi.org/10.1007/s00170-004-2363-5

[45] Shaba, A.A. (1996). Vibration of Continuous and Discrete Systems. Springer-Verlag New York, Inc.

[46] Campbell, S.L., Mayer, C.D. (2009). Generalized Inverses of Linear Transformations. SIAM.

[47] Yu, W., Li, X., Irwin, G.W. (2008). Stable anti-swing control for an overhead crane with velocity estimation and fuzzy compensation. In: Lowen, R., Verschoren, A. (eds.), Foundations of Generic Optimization, Applications of Fuzzy Control, Genetic Algorithms and Neural Networks, 2: 223-240. https://doi.org/10.1007/978-1-4020-6668-9_6

[48] Ioannou, P., Fidan, B. (2006). Adaptive Control Tutorial. SIAM. https://doi.org/10.1137/1.9780898718652

NOMENCLATURE

A_b	Cross-sectional area of beam, m^2
E_b	Young's modulus of beam, N/m^2
E_p	Young's modulus of piezo-material, N/m^2
f(x,t)	Excitation force, N
$H_{(.)}$	Heaviside step function
I_b	Moment of inertia of beam, kg/m^3
l_b	Length of beam, m
M_p	Piezo-moment per unit length, $N.m/m$
N	Number of mode shapes
N_a	Number of piezo-actuator
N_s	Number of piezo-sensor
t_b	Thickness of beam cross-section, m
t_p	Thickness of piezo cross-section, m
$v_a(t)$	Voltage of piezo-actuator, volt
w_b	Width of beam cross-section, m
w_p	Width of piezo cross-section, m
$x_{(.)}$	Location of piezo-actuators, m
y	Deflection of beam, m
C	$\in R^{N\times N}$, damping matrix, N.s/m
$e_{(.)}$	$\in R^{N}$, position error, m
g	$\in R^{N}$, excitation force vector, N
k	$\in R^{N\times N}$, stiffness matrix, N/m
K_d	$\in R^{N\times N}$, derivative gain matrix
K_χ	$\in R^{N\times N}$, proportional gain matrix
M	$\in R^{N\times N}$, mass matrix, kg
q	Modal displacement vector, m
Q	$\in R^{N\beta\times N\beta}$, adaptation matrix
W	$\in R^{N\beta\times N}$, weighting matrix
u	$\in R^{N}$, input vector, N
v_s	$\in R^{N_s}$ the piezo-sensor voltage vector, volt

Greek symbols

ρ_b	Density of beam, kg/m^3
β	Number of basis function terms
$\phi\ (x)$	Mode shape of beam
$\sigma_{(.)}$	$\in R^{N}$, sliding surface vector, m
α	$\in R^{N_s\times N}$, sensor gain matrix, m/volt
μ	$\in R^{N\times N_a}$, input coefficient matrix, N/volt
ξ	$\in R^{N}$, a lumped uncertain vector
φ	$\in R^{N\beta}$, basis function vector
χ	$\in R^{N}$, proxy position vector, m

Subscripts

b	beam
p	Piezo-material